

# Nonlinear Hall effect in topological Dirac semimetals in parallel magnetic field

Maxim Dzero,<sup>1</sup> Maxim Khodas,<sup>2</sup> Alex Levchenko,<sup>3</sup> and Vladyslav Kozii<sup>4</sup>

<sup>1</sup>*Department of Physics, Kent State University, Kent, Ohio 44242, USA*

<sup>2</sup>*The Racah Institute of Physics, The Hebrew University of Jerusalem, Jerusalem 91904, Israel*

<sup>3</sup>*Department of Physics, University of Wisconsin-Madison, Madison, Wisconsin 53706, USA*

<sup>4</sup>*Department of Physics, Carnegie Mellon University, Pittsburgh, Pennsylvania 15213, USA*

(Dated: August 29, 2025)

We compute the second-harmonic response of two-dimensional topological Dirac semimetals subjected to an in-plane magnetic field. The quantum kinetic equation for the Wigner distribution function is derived and then solved to compute the second-order electric-field contributions to the current density. Both the Berry curvature dipole and the field-induced terms in the current are analyzed across a broad range of model parameters. We propose that our theory can be tested experimentally by measuring the dependence of the anomalous Hall resistivity on the in-plane magnetic field in the surface states of the topological insulator SnTe, in WTe<sub>2</sub> and WSe<sub>2</sub> monolayers, as well as in the Kondo lattice material Ce<sub>3</sub>Bi<sub>4</sub>Pd<sub>3</sub> at very low temperatures.

## I. INTRODUCTION

Studies of the Hall effect have long held an important place in both experimental and theoretical condensed matter physics. In the conventional Hall effect, the transverse conductivity  $\sigma_{xy}$  describes the system's response to an external electric field and arises from the orbital motion of conduction electrons coupled to an external magnetic field [1]. In contrast, the anomalous Hall effect originates either from the Zeeman coupling of electrons to an external magnetic field or, in the absence of a field, from a nonzero net magnetization. In clean systems, the finite contribution to the anomalous Hall effect is determined by the Berry curvature of the Bloch wavefunctions, which modifies the electron velocity [2–9]. In both cases, however, it is evident that within linear response theory a nonzero Hall conductivity requires the breaking of time-reversal symmetry.

The next natural step in the study of the Hall effect has been to generalize the theory to nonlinear response [10–16]. In particular, it has been shown that a nonlinear Hall-like current can arise in systems lacking inversion symmetry, regardless of whether time-reversal symmetry is preserved [17–19]. This contribution to the conductivity is geometric in origin and is commonly referred to as the Berry curvature dipole (BCD) contribution [18, 20–30]. Most recently, it has also been theoretically proposed that the nonlinear Hall effect can be induced by superconducting fluctuations [31].

During the past few years several papers appeared reporting on the experimental observation of the nonlinear Hall effect in time-reversal invariant electronic systems [32–38]. Furthermore, giant nonlinear Hall effect has also been observed in an  $f$ -electron system Ce<sub>3</sub>Bi<sub>4</sub>Pd<sub>3</sub> [39]. What makes this material special is the presence of strong electronic correlations, which, thanks to the partially filled  $f$ -electronic orbitals on Ce ions, drive the formation of the local magnetic moments. It has been argued that this material belongs to the class of Weyl-Kondo semimetals [39, 40]. Although it was suggested that BCD may be responsible for the magnitude of the nonlinear Hall response, the onset of the effect below  $T^* \approx 3\text{K}$  still remains not fully understood [41, 42].

The intrinsic BCD contribution to the nonlinear Hall

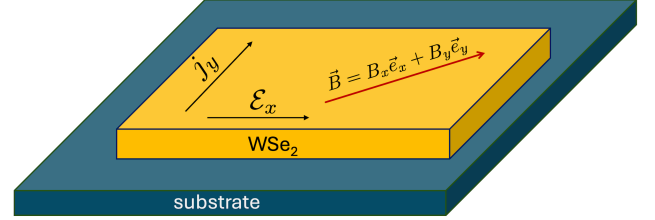


FIG. 1. Schematic representation of the experimental setup in which the electric field  $\mathcal{E}_x$  is applied along the  $x$ -axis of the two-dimensional metallic film (e.g., a single layer of WSe<sub>2</sub>) and electric current density  $j_y$  is measured along the  $y$ -axis. The external magnetic field is applied in the plane of the film. The application of magnetic field induces the nonlinear Hall response,  $j_y \propto \mathcal{E}_x^2$ . Nontrivial geometric properties of the underlying band structure also contribute to the nonlinear Hall effect whose magnitude is determined by the Berry curvature dipole. Depending on the direction of magnetic field as well as value of the microscopic model parameters, these two contributions may either enhance or cancel each other.

response necessarily requires that the corresponding crystal is described by one of the following point groups  $\{O, T, C_1, C_{1v}, C_{2v}, C_n, D_n\}$  with  $n = 1, 2, 3, 4, 6$  [18]. All of these point groups have a polar axis. For example, Ce<sub>3</sub>Bi<sub>4</sub>Pd<sub>3</sub> is described by the  $T_d$  point group which has  $C_3$  and  $C_2$  as its subgroups and therefore allows for nonzero Berry curvature dipole. More generally, in two-dimensional systems lacking inversion symmetry, the nonlinear Hall response can be tuned by an external in-plane magnetic field, as illustrated in Fig.1 [43–45]. Depending on its orientation, the field may either enhance or suppress the intrinsic contribution. The objective of the present work is to provide a detailed microscopic investigation of this effect.

In what follows, we consider a rather simple microscopic model of a two-dimensional disordered electronic system with the nontrivial geometric band structure which gives rise to both nonzero Berry curvature and BCD. Specifically, we will use the model of two tilted massive Dirac cones. To account for the effect of the in-plane magnetic field, we assume that the mass has a weak quadratic dispersion.

Using the theory of nonequilibrium systems, we derive the

quantum kinetic equation and compute the second-order response of the current density to an applied electric field in the presence of an in-plane magnetic field. Our approach enables the analysis of both the *ac*- and *dc*-limits. We further identify the conditions under which the magnetic-field contribution can become of the same order as the geometric Berry curvature dipole contribution.

Our paper is organized as follows. In the next section, we introduce the model and provide the details of the derivation of the quantum kinetic equation for the Wigner distribution function. In Section III, we present the calculation of the nonlinear contribution to the current density. In the first part of Section III, we analyze the nonlinear current in the absence of a magnetic field and re-derive the Berry curvature dipole contribution, while in the second part we examine the contribution arising from the external magnetic field. Section IV is devoted to a discussion of our results and conclusions. Finally, Appendices A, B, and C contain the technical details of the transport calculations. Throughout this work, we use units with  $\hbar = 1$ .

## II. MODEL AND FORMALISM

In this Section, we describe the formalism and provide the list of main equations which are used to calculate the second harmonic of the current density.

### A. Tilted massive Dirac fermion

We begin by considering the following two-band model Hamiltonian in two spatial dimensions [31, 46]:

$$\hat{H}_{\pm K}(\mathbf{k}) = \pm \alpha k_x \hat{\sigma}_0 + v k_x \hat{\sigma}_x \pm v k_y \hat{\sigma}_y + m \hat{\sigma}_z. \quad (1)$$

Pauli matrices  $\hat{\sigma}_i$  act in a space of underlying Kramers doublets and  $m$  determines the magnitude of the ferroelectric distortion [47, 48]. This Hamiltonian represents a minimal effective model for the surface states in crystalline topological insulator SnTe and monolayer WTe<sub>2</sub> as it describes electrons with dispersion determined by the two tilted massive Dirac cones located at momenta  $\pm K$  of the two-dimensional Brillouin zone, as shown in Fig. 2 [49–51]. Furthermore, we assume the scalar potential disorder  $U(\mathbf{r})$  with the white-noise Gaussian statistics  $\langle U(\mathbf{r})U(\mathbf{r}') \rangle_{\text{dis}} = \delta(\mathbf{r} - \mathbf{r}')/(2\pi\nu_F\tau)$ , where  $\tau^{-1}$  is the disorder scattering rate and  $\nu_F$  is the single-particle density of states per spin at the Fermi level. In the first part of this work, we will be interested in transport properties in the absence of a magnetic field, and for this reason it has not been included into Eq. (1). Lastly, parameter  $\alpha$  in Eq. (1) accounts for the tilt of the Dirac cones.

We find it convenient to work in the eigenbasis of Hamiltonian (1),  $\hat{H}_{sK}(\mathbf{k}) = \sum_{\eta=1}^2 \varepsilon_{\mathbf{k}s}^{(\eta)} |u_{s\eta}(\mathbf{k})\rangle \langle u_{s\eta}(\mathbf{k})|$ , where  $s = \pm 1$  is the valley index and the eigenenergies are given by

$$\varepsilon_{\mathbf{k}s}^{(\eta)} = s\alpha k_x + (-1)^\eta \sqrt{m^2 + v^2 k^2}. \quad (2)$$

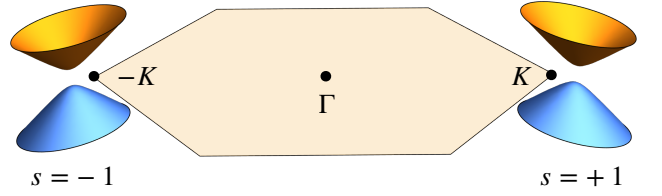


FIG. 2. Schematic low-energy band structure for monolayer WTe<sub>2</sub>. The two massive tilted Dirac cones are located at momenta  $\pm K$  in the hexagonal Brillouin zone, as described by Eq. (1), and  $s = \pm 1$  is the valley index.

The corresponding eigenvectors are

$$|u_{s1}(\mathbf{k})\rangle = \frac{1}{\sqrt{2}} \begin{pmatrix} -\sqrt{1 - \frac{m}{b_{\mathbf{k}}}} e^{-is\varphi_{\mathbf{k}}} \\ \sqrt{1 + \frac{m}{b_{\mathbf{k}}}} \end{pmatrix}, \quad (3)$$

$$|u_{s2}(\mathbf{k})\rangle = \frac{1}{\sqrt{2}} \begin{pmatrix} \sqrt{1 + \frac{m}{b_{\mathbf{k}}}} e^{-is\varphi_{\mathbf{k}}} \\ \sqrt{1 - \frac{m}{b_{\mathbf{k}}}} \end{pmatrix}.$$

Here we have introduced the shorthand notation  $b_{\mathbf{k}} = \sqrt{m^2 + v^2 k^2}$  and  $\tan \varphi_{\mathbf{k}} = k_y/k_x$ .

Next, we introduce the velocity operator which is defined according to  $\hat{v}_a^{(s)}(\mathbf{k}) = \partial_{k_a} \hat{H}_s(\mathbf{k})$ . Denoting  $\mathbf{n} = \mathbf{k}/k$ , the matrix elements of the velocity operator  $\hat{v}_x^{(s)}$  in the basis (3) are given by

$$\hat{v}_x^{(s)} = \begin{bmatrix} s\alpha - \frac{v^2 k_x}{b_{\mathbf{k}}} & \frac{v}{k} \left( -isk_y + \frac{mk_x}{b_{\mathbf{k}}} \right) \\ \frac{v}{k} \left( isk_y + \frac{mk_x}{b_{\mathbf{k}}} \right) & s\alpha + \frac{v^2 k_x}{b_{\mathbf{k}}} \end{bmatrix}. \quad (4)$$

Similarly, for the matrix elements of the velocity operator  $\hat{v}_y^{(s)}$  we have

$$\hat{v}_y^{(s)} = \begin{bmatrix} -\frac{v^2 k_y}{b_{\mathbf{k}}} & \frac{v}{k} \left( isk_x + \frac{mk_y}{b_{\mathbf{k}}} \right) \\ \frac{v}{k} \left( -isk_x + \frac{mk_y}{b_{\mathbf{k}}} \right) & \frac{v^2 k_y}{b_{\mathbf{k}}} \end{bmatrix}. \quad (5)$$

It is well known that the band structure described by Eq. (1) possesses nontrivial geometric phase. Introducing the Berry connection  $\vec{\mathcal{A}}^{(\eta)}(\mathbf{k}) = i\langle \eta\mathbf{k} | \vec{\nabla}_{\mathbf{k}} | \eta\mathbf{k} \rangle$  and the Berry curvature  $\Omega_a^{(\eta)}(\mathbf{k}) = \epsilon^{abc} \partial_b \mathcal{A}_c^{(\eta)}(\mathbf{k})$ , we find that  $\Omega_x^{(\eta)} = \Omega_y^{(\eta)} = 0$  and

$$\Omega_z^{(\eta)}(\mathbf{k}) = \left( \frac{smv^2}{2b_{\mathbf{k}}^3} \right) (-1)^{1+\eta}. \quad (6)$$

As one may have expected, the Berry curvature is independent of the tilt parameter  $\alpha$  and is proportional to the energy gap in the Dirac spectrum and the valley index. The latter turns out to be crucial for nonlinear Hall effect.

### B. Quantum kinetic equation

The key quantity in our subsequent analysis is the Wigner distribution function (WDF) which is defined according to

$$w_{\alpha\beta}(\vec{k}, \vec{r}; \epsilon, t) = \frac{1}{2\pi} \int d^2\vec{\rho} \int d\eta e^{i\vec{k}\vec{\rho} - i\epsilon\eta} \times \left\langle \psi_\beta^\dagger \left( \vec{r} + \frac{\vec{\rho}}{2}, t + \frac{\eta}{2} \right) \psi_\alpha \left( \vec{r} - \frac{\vec{\rho}}{2}, t - \frac{\eta}{2} \right) \right\rangle. \quad (7)$$

Here  $\psi_\alpha^\dagger(\mathbf{r}, t)$  and  $\psi_\alpha(\mathbf{r}, t)$  are the usual creation and annihilation fermionic fields for a given valley and averaging is performed over the ground state of the Hamiltonian (1). Spatial homogeneity of WDF is restored after averaging over disorder. In the absence of external fields, we find for the WDF computed in the basis of Eq. (3):

$$\hat{w}_{\mathbf{k}\epsilon}^{(0)} = f(\epsilon) \begin{pmatrix} \delta(\epsilon - \epsilon_{\mathbf{k}s}^{(1)}) & 0 \\ 0 & \delta(\epsilon - \epsilon_{\mathbf{k}s}^{(2)}) \end{pmatrix}, \quad (8)$$

where  $f(\epsilon)$  is the Fermi-Dirac distribution function. In the presence of a spatially uniform electric field, the WDF satisfies the following quantum kinetic equation [52, 53]

$$\left( \frac{\partial}{\partial t} + \frac{1}{\tau} \right) \hat{w}_{\mathbf{k}\epsilon}(t) + i[\mathbf{b}_{\mathbf{k}} \cdot \boldsymbol{\sigma}, \hat{w}_{\mathbf{k}\epsilon}(t)]_- = -\alpha \tilde{\nabla}_x \hat{w}_{\mathbf{k}\epsilon}(t) - \frac{v}{2} \{ \hat{\sigma}, \tilde{\nabla} \hat{w}_{\mathbf{k}\epsilon}(t) \}_+. \quad (9)$$

Here  $\{\hat{f}, \hat{g}\}_\pm = \hat{f}\hat{g} \pm \hat{g}\hat{f}$  and

$$\tilde{\nabla} \hat{w}_{\mathbf{k}\epsilon}(t) = \frac{e\mathbf{E}(t)}{\omega} \left( \hat{w}_{\mathbf{k}\epsilon + \frac{\omega}{2}}(t) - \hat{w}_{\mathbf{k}\epsilon - \frac{\omega}{2}}(t) \right). \quad (10)$$

In the kinetic equation (9), we have also neglected the collision integral beyond  $\tau$ -approximation, which is technically equivalent to neglecting vertex corrections due to disorder scattering. In the limit when electric field is weak, kinetic equation (9) can be solved by perturbation theory. For example, for the monochromatic electric field  $\mathbf{E}(t) = \vec{\mathcal{E}} e^{i\omega t} + \text{c.c.}$ , the first order correction to the WDF is

$$\begin{aligned} [\hat{w}_{\mathbf{k}\epsilon}^{(1)}]_{aa} &= - \left( \frac{e}{\omega z_\omega} \right) ([\hat{\mathbf{v}}]_{aa} \cdot \vec{\mathcal{E}}) \left( \hat{w}_{\mathbf{k}\epsilon + \frac{\omega}{2}}^{(0)} - \hat{w}_{\mathbf{k}\epsilon - \frac{\omega}{2}}^{(0)} \right)_{aa}, \\ [\hat{w}_{\mathbf{k}\epsilon}^{(1)}]_{a\bar{a}} &= - \left( \frac{e Z_{\mathbf{k}\omega}^{(a)}}{2\omega} \right) ([\hat{\mathbf{v}}]_{a\bar{a}} \cdot \vec{\mathcal{E}}) \sum_{b=1}^2 \left( \hat{w}_{\mathbf{k}\epsilon + \frac{\omega}{2}}^{(0)} - \hat{w}_{\mathbf{k}\epsilon - \frac{\omega}{2}}^{(0)} \right)_{bb}, \end{aligned} \quad (11)$$

where  $a = (1, 2)$ ,  $\bar{1} = 2$ ,  $\bar{2} = 1$ ,  $z_\omega = -i\omega + \tau^{-1}$  and  $Z_{\mathbf{k}\omega}^{(a)} = [z_\omega + 2ib_{\mathbf{k}} \cos(\pi a)]^{-1}$ .

### III. NONLINEAR RESPONSE

Given the Wigner distribution function, the current density can be computed as

$$\mathbf{j}(t) = -e \int \frac{d^2\mathbf{k}}{(2\pi)^2} \int_{-\infty}^{\infty} \text{Tr}[\hat{\mathbf{v}} \hat{w}_{\mathbf{k}\epsilon}(t)] d\epsilon, \quad (12)$$

where  $\hat{v}_x$  and  $\hat{v}_y$  are the  $x$ - and  $y$ -components of the velocity operator with the matrix elements given by Eqs. (4,5). We reproduce *linear* intrinsic contribution to the anomalous Hall effect in Appendix A.

#### A. Berry curvature dipole contribution

Before analyzing the role of the in-plane magnetic field, we first demonstrate the microscopic derivation of the geometric contribution to the second harmonic using the method of quantum kinetic equation. This contribution is determined by the Berry curvature dipole, which in two dimensions is defined as [18]

$$\mathcal{D}_i \equiv 4 \int \frac{d^2\mathbf{k}}{(2\pi)^2} \Omega_z(\mathbf{k}) \frac{\partial f(\epsilon_{\mathbf{k}s})}{\partial k_i}, \quad (13)$$

with  $i = x, y$ . We find that it is proportional to the tilt parameter  $\alpha$ , Eq. (1).

Given our choice of the model, the Berry curvature dipole will be pointing along the  $x$ -axis (see Eq. (23) below). We find it more convenient to consider the situation when electric field lies in the  $xy$ -plane and compute the current along the  $x$ -axis. In this case the nonlinear Hall contribution to the current is defined by

$$j_x^{(2\omega)} = \chi_{xxy}(\omega) \mathcal{E}_x \mathcal{E}_y. \quad (14)$$

An interesting property of the quantum kinetic equation (9) is that the second order corrections to the WDF are formally given by the same expressions as the first order ones, Eq. (11), in which we replace  $\hat{w}_{\mathbf{k}\epsilon}^{(0)} \rightarrow \hat{w}_{\mathbf{k}\epsilon}^{(1)}$ . Straightforward analysis shows that the contribution to  $\chi_{xxy}$  from the diagonal matrix elements of the velocity operator and WDF given by  $[\hat{v}_x]_{11}[\hat{w}_{\mathbf{k}\epsilon}^{(2)}]_{11} + [\hat{v}_x]_{22}[\hat{w}_{\mathbf{k}\epsilon}^{(2)}]_{22} \propto s\alpha k_x^2$  which gives zero upon the summation over valleys,  $s = \pm$ . We therefore conclude that nonlinear correction to the current must originate from the processes which involve the off-diagonal matrix elements of the WDF.

We therefore analyze the remaining contribution  $[\hat{v}_x]_{12}[\hat{w}_{\mathbf{k}\epsilon}^{(2)}]_{21} + [\hat{v}_x]_{21}[\hat{w}_{\mathbf{k}\epsilon}^{(2)}]_{12}$ . With the help of expressions for  $[\hat{w}_{\mathbf{k}\epsilon}^{(2)}]_{a\bar{a}}$  (see Appendix C for details), we find that the combination of velocity matrix elements  $[\hat{v}_x]_{12}[\hat{v}_x]_{21}[\hat{v}_x]_{aa} \propto k_y$  gives zero upon integration over  $k_y$ . Therefore, the only nonzero contribution will arise from the following combinations:  $[\hat{v}_y]_{12}[\hat{v}_x]_{21}[\hat{v}_x]_{aa}$  and  $[\hat{v}_x]_{12}[\hat{v}_y]_{21}[\hat{v}_x]_{aa}$ . In particular, with the help of expressions (4,5), we find

$$\begin{aligned} [\hat{v}_y]_{21}[\hat{v}_x]_{12} &= -\frac{ismv^2}{b_{\mathbf{k}}} - \frac{v^2 k_x k_y}{b_{\mathbf{k}}^2}, \\ [\hat{v}_y]_{12}[\hat{v}_x]_{21} &= \frac{ismv^2}{b_{\mathbf{k}}} - \frac{v^2 k_x k_y}{b_{\mathbf{k}}^2}. \end{aligned} \quad (15)$$

Again keeping in mind the subsequent integrations over momentum components, one realizes that the terms  $\propto k_x k_y$  do not contribute to the second harmonic since the resulting expression under the integral will depend only on  $k_x$  and  $k_x^2 + k_y^2$ . As

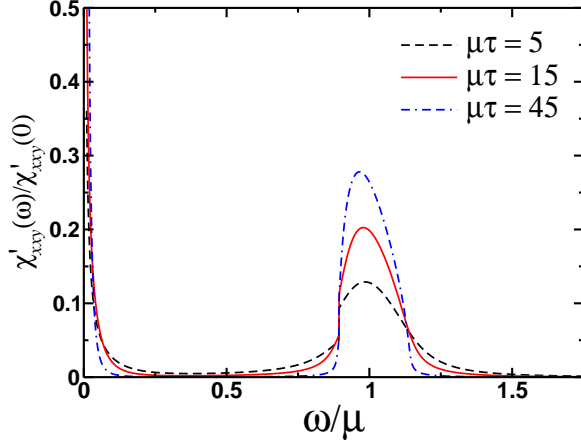


FIG. 3. Frequency dependence of the real part of the nonlinear response function (16) for different values of the disorder scattering rate. In order to generate this plot we used  $\alpha/v = 0.125$  and  $m/\mu = 0.33$ .

a result, we derive the following expression for the response function  $\chi_{xy}$ :

$$\chi_{xy} = \left( \frac{2e^3}{\omega^2 z_\omega} \right) \sum_{s=\pm} \int \frac{d^2 \mathbf{k}}{(2\pi)^2} \left( \frac{smv^3}{z_{2\omega}^2 + 4b_{\mathbf{k}}^2} \right) \times \int_{-\infty}^{\infty} \left( \frac{vk_x}{b_{\mathbf{k}}} \right) \mathcal{W}(\mathbf{k}\epsilon; \omega) d\epsilon, \quad (16)$$

where function  $\mathcal{W}(\mathbf{k}\epsilon; \omega)$  is defined according to

$$\mathcal{W}(\mathbf{k}\epsilon; \omega) = \sum_{a=1}^2 (-1)^a \left[ \hat{w}_{\mathbf{k}\epsilon+\omega}^{(0)} + \hat{w}_{\mathbf{k}\epsilon-\omega}^{(0)} - 2\hat{w}_{\mathbf{k}\epsilon}^{(0)} \right]_{aa}. \quad (17)$$

Equation (16) is derived in the limit  $\alpha \ll v$  and ignores contributions of order  $O(\alpha^2)$ . In Fig. 3, we present the frequency dependence of the real part of the response function,  $\chi_{xy}(\omega) = \chi'_{xy}(\omega) + i\chi''_{xy}(\omega)$ . Notably, function  $\chi'_{xy}(\omega)$  exhibits a peak at frequency  $\omega \approx \mu$ . This peak describes the resonant transitions between the valence and conduction band. The location of the peak is deduced from the fact that the denominator in the expression under the integral (16) approaches zero as  $\tau \rightarrow \infty$ . This resonant effect is not captured by the semiclassical Boltzmann equation approach [18] (see also [54] and references therein).

*a. Low frequency limit.* We consider the limit of low frequencies first. Specifically, we take  $\omega \ll m$  and for weak disorder  $m\tau \gg 1$  we have  $z_{2\omega} \ll 2b_{\mathbf{k}}$ , so that the expression under the integral (16) simplifies to

$$\chi_{xy} \approx \sum_{s=\pm} \left( \frac{e^3 v^4}{2\omega^2} \right) \left( \frac{sm}{z_\omega} \right) \int \frac{d^2 \mathbf{k}}{(2\pi)^2} \frac{k_x}{b_{\mathbf{k}}^3} \times [f(\epsilon_{\mathbf{k}s} + \omega) + f(\epsilon_{\mathbf{k}s} - \omega) - 2f(\epsilon_{\mathbf{k}s})]. \quad (18)$$

Here we assumed for definiteness that the chemical potential lies in the upper band,  $\mu > 0$ . Expanding the distribution

functions in powers of  $\omega$  yields

$$\chi_{xy} \approx \sum_{s=\pm} \frac{sm e^3 v^2 \tau}{2(1 - i\omega\tau)} \int \frac{d^2 \mathbf{k}}{(2\pi)^2} \frac{v^2 k_x}{b_{\mathbf{k}}^3} f''(\epsilon_{\mathbf{k}s}). \quad (19)$$

Next, we express function  $\chi_{xy}$  explicitly in terms of the integral over the Berry curvature. To do that we replace the expression under the integral using the following identity

$$\frac{v^2 k_x}{b_{\mathbf{k}}} f''(\epsilon_{\mathbf{k}}) = \frac{\partial}{\partial k_x} f'(\epsilon_{\mathbf{k}s}) - s\alpha f''(\epsilon_{\mathbf{k}s}). \quad (20)$$

At this point it will be convenient to separate the contributions from different valleys, so we write  $\chi_{xy} = \sum_{s=\pm} \chi_{xy}^{(s)}$  with

$$\chi_{xy}^{(s)} = \frac{sm e^3 v^2 \tau}{2(1 - i\omega\tau)} \int \frac{d^2 \mathbf{k}}{(2\pi)^2} \frac{1}{b_{\mathbf{k}}^2} \frac{\partial}{\partial k_x} [f'(\epsilon_{\mathbf{k}s})] - \frac{m\alpha e^3 v^2 \tau}{2(1 - i\omega\tau)} \int \frac{d^2 \mathbf{k}}{(2\pi)^2} \frac{1}{b_{\mathbf{k}}^2} f''(\epsilon_{\mathbf{k}s}). \quad (21)$$

Integrating by parts in the first term and using Eq. (20) again we find:

$$\chi_{xy}^{(s)} = \frac{e^3 \tau}{(1 - i\omega\tau)} \int \frac{d^2 \mathbf{k}}{(2\pi)^2} \left( \frac{smv^2}{b_{\mathbf{k}}^3} \right) \frac{\partial f(\epsilon_{\mathbf{k}s})}{\partial k_x} - \frac{m\alpha e^3 v^2 \tau}{2(1 - i\omega\tau)} \int \frac{d^2 \mathbf{k}}{(2\pi)^2} \left\{ \frac{f'(\epsilon_{\mathbf{k}s})}{b_{\mathbf{k}}^3} + \frac{f''(\epsilon_{\mathbf{k}s})}{b_{\mathbf{k}}^2} \right\}. \quad (22)$$

Let us first consider the first term in Eq. (22). Given the expressions for the Berry curvature, Eq. (6), and the Berry curvature dipole, Eq. (13), one immediately recognizes that the first integral in Eq. (22) is of geometric origin:

$$\chi_{xy}^{(s)} = \frac{e^3 \tau}{(1 - i\omega\tau)} \int \frac{d^2 \mathbf{k}}{(2\pi)^2} \left( \frac{smv^2}{b_{\mathbf{k}}^3} \right) \frac{\partial f(\epsilon_{\mathbf{k}s})}{\partial k_x} \equiv \frac{e^3 \tau \mathcal{D}_x}{4(1 - i\omega\tau)}, \quad (23)$$

where we calculated for the Berry curvature dipole

$$\mathcal{D}_x = \frac{3\alpha m |\mu| \gamma^2 v^3 (v^2 - \alpha^2)}{\pi (\mu^2 v^2 + m^2 \alpha^2)^{5/2}} \quad (24)$$

and we defined the parameter  $\gamma = \sqrt{\mu^2 v^2 / (v^2 - \alpha^2) - m^2}$ . To the leading order in  $\alpha$ , this contribution does not depend on the valley index  $s = \pm 1$  and, as a result, subsequent summation over valleys yields  $\chi_{xy} = e^3 \tau \mathcal{D}_x / 2(1 - i\omega\tau)$ . For details of the evaluation of the momentum integral in Eq. (23) we refer the reader to Appendix B.

As for the remaining integral in Eq. (22), one notices that it is proportional to  $\alpha$  and after subsequent rearrangement of the terms it will give the contribution  $O(\alpha^2)$  which we ignore. In principle, it can be shown that this contribution will exactly cancel the corresponding contribution from the similar term in Eq. (16), which we have ignored as well. This cancellation is not accidental and is guaranteed by the time-reversal symmetry of the system.

Equation (24) represents the only nonzero component of the Berry curvature dipole. Indeed, as expected on purely symmetry grounds, we find that the second harmonic response

is linearly proportional to the tilt parameter  $\alpha$  which breaks the mirror symmetry and gives rise to nonzero Berry curvature dipole contribution  $\vec{\mathcal{D}} = \mathcal{D}_x \vec{e}_x$ . Finally, in the dc limit,  $\omega\tau \ll 1$ , and assuming also  $v \gg \alpha$ ,  $\mu \gg m$ , we find for the response function after summation over the two valleys

$$[\chi_{xy}]_{\omega\tau \ll 1} \approx \left( \frac{3e^3}{2\pi} \right) \frac{m\alpha\tau}{\mu^2}. \quad (25)$$

The calculation presented above can of course be repeated assuming the electric field is aligned along the  $x$ -axis, while the current is flowing along the  $y$ -axis, i.e., only the  $y$ -components of the velocity operator in Eq. (12) needs to be considered. As a result, the general expression for the nonlinear current can be written as

$$\vec{j}_{2\omega} = \frac{e^3 \tau (\vec{\mathcal{D}} \cdot \vec{\mathcal{E}})}{2(1 - i\omega\tau)} (\vec{\mathcal{E}} \times \vec{e}_z). \quad (26)$$

Absolutely analogous expression can be derived for the dc second-order current, with  $(\vec{\mathcal{E}} \times \vec{e}_z)$  replaced by  $(\vec{\mathcal{E}}^* \times \vec{e}_z)$ .

*b. High frequency limit.* We now turn our attention to the analysis of  $\chi_{xy}(\omega)$ , Eq. (16), in the limit of high frequencies,  $\omega \sim m$  and  $\omega\tau \gg 1$  while keeping  $\omega \ll \mu$ . The latter condition still allows us to expand the arguments of the distribution functions up to the second order in powers of  $\omega/\mu$ . The remaining part of the calculation is very similar to that leading us to Eq. (22). As a result, we find that at high frequencies

$$[\chi_{xy}]_{\omega\tau \gg 1} \sim \frac{im\alpha}{\omega\mu^2}, \quad (27)$$

which is purely dissipative.

As the frequency increases, the second-order response exhibits a sharp resonance around  $\omega \approx \mu$ , as shown in Fig. 3. At even higher frequencies,  $\omega \gg \mu$ , we find that  $[\chi_{xy}]_{\omega\tau \gg 1} \sim i/\omega^3$ .

## B. Effect of in-plane magnetic field

As we have discussed so far, Eq. (26) represents the only nonzero second-order Hall response without an external magnetic field  $\mathbf{B}$ . In order to elucidate the contribution from an in-plane magnetic field, we assume that it couples to spin  $\hat{\sigma}$  through the Zeeman coupling and modify the model Hamiltonian as follows

$$\hat{\mathcal{H}}_{\pm K}(\mathbf{k}) = \hat{H}_{\pm K}(\mathbf{k}) - g\mu_B(B_x \hat{\sigma}_x + B_y \hat{\sigma}_y) + \frac{\beta k^2}{2} \hat{\sigma}_z, \quad (28)$$

where  $g$  is the gyromagnetic factor and  $\mu_B$  is Bohr's magneton.

It is important to note that the minimal Zeeman coupling in Eq. (28) was written treating the matrices  $\hat{\sigma}_{x,y}$  as if they directly represented spin components. In reality, however, this Hamiltonian describes an effective low-energy model in which  $\hat{\sigma}_{x,y}$  incorporate admixtures of both spin and orbital degrees of freedom. As a result, upon projecting onto the two lowest-energy bands, the effective  $g$ -factor acquires a nontrivial  $\mathbf{k}$ -dependence, the precise form of which depends on microscopic details. In this work, we neglect that momentum

dependence and treat  $g$  as a constant, anticipating that this approximation does not qualitatively affect our main results.

Expressions for the basis functions can be easily generalized by noting that in the absence of the tilt and mass dispersion the effect of magnetic field results in the shift of momentum :

$$k_x \rightarrow q_x = k_x - \frac{g\mu_B}{v} B_x, \quad k_y \rightarrow q_y = k_y - \frac{g\mu_B}{v} B_y. \quad (29)$$

The mass dispersion in Eq. (28),  $\beta k^2 \hat{\sigma}_z/2$ , which is naturally present in realistic materials, is crucial for our analysis. As we demonstrate below, the leading field-dependent contribution to the second harmonic is proportional to  $\chi_{xy} \propto \alpha(\beta B)^2$ , to the lowest order in the magnetic field. In principle, we could have also considered nonlinear-in-momentum corrections to the Dirac dispersion, however, while amenable to a numerical analysis, producing analytically tractable calculations for this case turns out to be quite challenging.

Primarily for computational convenience, we consider the setup in which the direction of the electric field points along the  $x$ -axis,  $\vec{\mathcal{E}} = \mathcal{E}_x \vec{e}_x$ , and compute the first and second harmonics of the current along the  $y$ -axis, see Fig. 1. The weakly dispersive mass term modifies the velocity operators according to

$$\hat{v}_x^{(s)} = \begin{bmatrix} s\alpha - \frac{v^2 q_x}{b_q} - \frac{\beta m_k k_x}{b_q} & \frac{v}{q} \left( -isq_y + \frac{m_k q_x}{b_q} - \frac{\beta q^2 k_x}{b_q} \right) \\ \frac{v}{q} \left( isq_y + \frac{m_k q_x}{b_q} - \frac{\beta q^2 k_x}{b_q} \right) & s\alpha + \frac{v^2 q_x}{b_q} + \frac{\beta m_k k_x}{b_q} \end{bmatrix} \quad (30)$$

and

$$\hat{v}_y^{(s)} = \begin{bmatrix} -\frac{v^2 q_y}{b_q} - \frac{\beta m_k k_y}{b_q} & \frac{v}{q} \left( isq_x + \frac{m_k q_y}{b_q} - \frac{\beta q^2 k_y}{b_q} \right) \\ \frac{v}{q} \left( -isq_x + \frac{m_k q_y}{b_q} - \frac{\beta q^2 k_y}{b_q} \right) & \frac{v^2 q_y}{b_q} + \frac{\beta m_k k_y}{b_q} \end{bmatrix}. \quad (31)$$

Here we introduced  $q = \sqrt{(k_x - g\mu_B B_x/v)^2 + (k_y - sg\mu_B B_y/v)^2}$ ,  $m_k = m + \beta k^2/2$ , and  $b_q = (v^2 q^2 + m_k^2)^{1/2}$ . In what follows, we will be focusing solely on contributions from the magnetic field.

*a. Second order corrections.* We proceed by looking at the contribution from the second-order (in electric field) corrections to the *diagonal* components of the WDF. Taking into account that the chemical potential lies in the conduction band, we only need to consider the contribution from the conduction band ( $a = 2$  in the expressions below). After a simple calculation, it follows that

$$\sum_{a=1}^2 [\hat{v}_y^{(s)}]_{aa} [\hat{w}_{\mathbf{k}\epsilon}^{(2)}]_{aa} \propto \left( \frac{e^2}{\omega^2 z_{\omega} z_{2\omega}} \right) [\hat{v}_y^{(s)}]_{22} [\hat{v}_x^{(s)}]_{22} [\hat{v}_x^{(s)}]_{22} + \left( \frac{e^2 z_{\omega}}{2\omega^2 z_{2\omega}} \right) \frac{([\hat{v}_y^{(s)}]_{11} + [\hat{v}_y^{(s)}]_{22}) [\hat{v}_x^{(s)}]_{12} [\hat{v}_x^{(s)}]_{21}}{z_{\omega}^2 + 4b_q^2}. \quad (32)$$

The second term in Eq. (32) vanishes identically since  $\hat{v}_y^{(s)}$  is a traceless matrix. The analysis of the first term must be done carefully, bearing in mind that the  $y$ -component of the magnetic field enters in combination with the valley index  $s$  (see Eq. (29)). This implies that the terms which ultimately

may produce nonzero magnetic field contribution to the second harmonic must be necessarily proportional to the product of  $s\alpha$  and  $k_y = q_y + sg\mu_B B_y/v$ . After going through all possible combinations, we find that expression (32) produces only one term which does not vanish upon momentum integration and summation over the valley index  $s$ . It is given by

$$[j_y^{(2\omega)}]_{\text{diag.}} = \left( \frac{4e^3\alpha\beta^2}{\omega^2 z_{2\omega} z_{2\omega}} \right) \int \frac{d^2\mathbf{q}}{(2\pi)^2} \frac{m_{\mathbf{k}}^2}{b_{\mathbf{q}}^2} k_x k_y \quad (33)$$

$$\times [2\theta(\mu - b_{\mathbf{q}}) - \theta(\mu + \omega - b_{\mathbf{q}}) - \theta(\mu - \omega - b_{\mathbf{q}})] \mathcal{E}_x^2,$$

where we redefine  $k_{x,y} = q_{x,y} + g\mu_B B_{x,y}/v$ . The summation over the valley index  $s$  has already been performed, and we have changed the integration variables from  $\mathbf{k}$  to  $\mathbf{q}$ . The functions  $b_{\mathbf{q}}$  and  $m_{\mathbf{k}}$  are defined below Eq. (31), and  $\mathbf{k}$  should now be viewed as a function of  $\mathbf{q}$ . One observes that the Hall current acquires a maximum value when the magnetic field points at a  $\pi/4$  angle with respect to the direction of the electric field. We note that the low-field expansion of the second harmonic starts with the second power of the magnetic field, even though the contribution from a single valley is linear.

For small values of the magnetic field  $\mathbf{B}$  and parameter  $\beta$ ,  $\max\{\beta g^2 \mu_B^2 B^2/v^2, \beta k_F^2\} \ll m$ , we can ignore the dependence of  $m_{\mathbf{q}}$  on momentum. In this case, assuming also that  $\omega \ll \mu$ , the integral in Eq. (33) evaluates to  $(m\omega)^2/2\pi(v\mu)^2$ , so that for Eq. (33) we find approximately (at  $\omega\tau \ll 1$ )

$$[j_y^{(2\omega)}]_{\text{diag.}} \approx 2 \left( \frac{e^3\alpha}{\pi} \right) \left( \frac{g\mu_B}{\mu} \right)^2 \left( \frac{\beta}{v^2} \right)^2 (m\tau)^2 B_x B_y \mathcal{E}_x^2. \quad (34)$$

Comparing this result with Eq. (25), we see that the relative magnitude of the magnetic-field-induced Hall current is determined by the value of the dimensionless parameter

$$\eta = \frac{4}{3} \left( \frac{m\beta}{v^2} \right)^2 \left( \frac{g\mu_B}{m} \right)^2 m\tau B_x B_y. \quad (35)$$

Clearly, in a sufficiently clean material and strong magnetic field parameter  $\eta$  can be of the order  $O(1)$ .

We proceed with evaluating the contribution from the *off-diagonal* components of the WDF,  $\sum_{a=1}^2 [\hat{v}_y^{(s)}]_{\bar{a}\bar{a}} [\hat{u}_{\mathbf{k}_e}^{(2)}]_{\bar{a}\bar{a}}$ . Since we have already assumed that the chemical potential lies in the conduction band, the evaluation of this contribution reduces to the analysis of the following combinations of the velocity matrix elements:  $[\hat{v}_y^{(s)}]_{12} [\hat{v}_x^{(s)}]_{21} [\hat{v}_x^{(s)}]_{22}$  and  $[\hat{v}_y^{(s)}]_{21} [\hat{v}_x^{(s)}]_{12} [\hat{v}_x^{(s)}]_{22}$ . Similarly, we find that the only nonzero contribution to the second harmonic will be given by the following expression:

$$[j_y^{(2\omega)}]_{\text{off.}} = \left( \frac{2e^3 z_{2\omega}}{\omega^2 z_{2\omega}} \right) \alpha \beta^2 \int \frac{d^2\mathbf{q}}{(2\pi)^2} \frac{k_x k_y v^2 q^2}{b_{\mathbf{q}}^2 (z_{2\omega}^2 + 4b_{\mathbf{q}}^2)} \quad (36)$$

$$\times [2\theta(\mu - b_{\mathbf{q}}) - \theta(\mu + \omega - b_{\mathbf{q}}) - \theta(\mu - \omega - b_{\mathbf{q}})] \mathcal{E}_x^2,$$

and  $k_{x,y}$  are functions of  $q_{x,y}$ , correspondingly, see below Eq. (33).

In the general case, Eq. (36) needs to be analyzed numerically. However, assuming small  $B$  and  $\beta$ , it can be analytically evaluated under the exactly same assumptions that led to

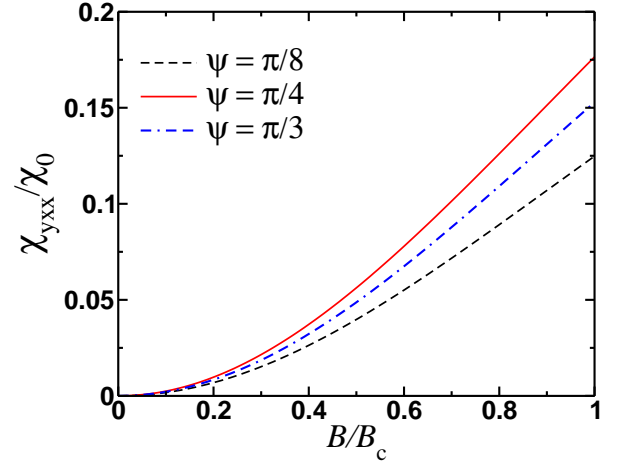


FIG. 4. Magnetic-field-dependent contribution to the second-order Hall conductivity  $\chi_{yxx} \equiv j_y^{(2\omega)}/\mathcal{E}_x^2$ , given by the sum of Eqs. (33) and (36). Here  $\psi$  is the angle between the magnetic field  $\mathbf{B}$  and the  $x$ -axis,  $\chi_0 = (e^3\alpha/\mu^2)(\beta k_F^2\tau)^2$  and  $B_c = vk_F/g\mu_B$ . We stress that the response function increases until the magnetic field reaches the critical value  $B_{\text{max}}$  given by Eq. (39). At  $B > B_{\text{max}}$ , the kinematic constraints cannot be satisfied and the response function decreases to zero.

Eq. (34). In this limit, we find

$$[j_y^{(2\omega)}]_{\text{off.}} \approx \left( \frac{e^3\alpha}{\pi} \right) \left( \frac{g\mu_B}{\mu} \right)^2 \left( \frac{\beta}{v^2} \right)^2 B_x B_y \mathcal{E}_x^2. \quad (37)$$

This expression differs from (34) by the dimensionless prefactor  $(m\tau)^2$ , so that in the case  $m\tau \gg 1$  the intraband contribution to the second harmonic dominates the interband one, Eq. (37). In contrast, in the disordered case,  $m\tau \ll 1$  and  $\omega\tau \ll 1$ , the situation is reversed, and the interband contribution becomes dominant.

Combining the two contributions (34) and (37) together, we find in the low-field limit

$$j_y^{(2\omega)} = [j_y^{(2\omega)}]_{\text{diag.}} + [j_y^{(2\omega)}]_{\text{off.}} \quad (38)$$

$$\approx \left( \frac{e^3\alpha}{\pi} \right) \left( \frac{g\mu_B}{\mu} \right)^2 \left( \frac{\beta}{v^2} \right)^2 [1 + 2(m\tau)^2] B_x B_y \mathcal{E}_x^2.$$

We stress that while the chemical potential  $\mu$  can be directly controlled by the metallic gate, the in-plane magnetic field does not change it even in systems with a fixed number of particles.

In Fig. 4, we present the results of the numerical calculation of the dependence of the response function  $\chi_{yxx}(B) \equiv |j_y^{(2\omega)}(B)|/\mathcal{E}_x^2$ , with  $j_y^{(2\omega)}(B)$  given by the sum of Eqs. (33) and (36), on the magnitude of an external magnetic field. As expected, for small fields  $g\mu_B B \ll \mu$  we find that the function  $\chi_{yxx}(B)$  grows quadratically with the magnetic field. As the value of the magnetic field increases further, one observes that the kinematic constraints imposed by the step-functions cannot be satisfied and the second harmonic decreases to zero. The value of the magnetic field  $B_{\text{max}}$  when this happens can



be found from the condition  $\mu + \omega = b_{q=0}$  which yields

$$g\mu_B B_{\max} = \sqrt{\frac{2v^2}{\beta}(\mu + \omega - m)}. \quad (39)$$

For  $B \sim B_{\max}$  it follows that  $\chi_{y,xx}(B < B_{\max})$  increases linearly with magnetic field. However, given that in realistic experimental situation  $v^2/\beta \gg \mu$ , we do not expect that this scale can be probed experimentally.

It is worth mentioning here that if one decides to consider the setup in which the current flows along the  $x$ -axis, one also finds that  $j_x^{(2\omega)}/(\mathcal{E}_x \mathcal{E}_y) \propto B_x B_y$ . In such a setup, it is this term which will be added to the corresponding contribution from the BCD, Eq. (14).

#### IV. DISCUSSION AND CONCLUSIONS

In addition to the intrinsic contribution from the Berry curvature dipole discussed in this work, realistic materials also exhibit extrinsic mechanisms – such as side-jump and skew-scattering processes – that can contribute comparably to the nonlinear Hall response [16, 55, 56]. Although we did not include disorder-assisted effects in our analysis, we expect the predicted dependence of the nonlinear Hall effect on the magnetic field direction to remain robust and observable at sufficiently high fields. A detailed investigation of these extrinsic contributions is left for future work.

To estimate the magnitude of the effect studied in this work, we use Eq. (35) that determines the ratio between the magnetic field and the Berry curvature dipole contributions to the nonlinear Hall response. In a disordered system ( $m\tau \sim 1$ ) this parameter is quite small. However, in a relatively clean electronic system the smallness of the energy scale  $\beta(g\mu_B B/v)^2$  can be partially compensated by the large value of  $m\tau$ . For example, in  $\text{WSe}_2$  and  $\text{WTe}_2$  monolayers we can estimate  $m \approx 10$  meV,  $\beta k_F^2 \approx 80$  meV and  $\hbar/\tau \approx 1$  meV [54], which yields  $\hbar/(m\tau) \approx 0.1$  and  $\eta \approx 3(g\mu_B B/m)^2$ . For magnetic fields in the range  $B \sim 1 \div 10$  T, we find  $\eta \sim 0.03 \div 0.3$ , which is experimentally observable. The situation for  $\text{Ce}_3\text{Bi}_4\text{Pd}_3$  seems even more favorable, as the electron's velocity is significantly reduced due to the strong hybridization between the conduction and  $f$ -electrons of the cerium ions.

Finally, we highlight the advantages of the quantum kinetic equation approach employed in this work. Unlike the semiclassical Boltzmann formalism, this method provides a unified framework that remains valid across a wide range of frequencies, magnetic field strengths, and chemical potential values. It also naturally incorporates various forms of disorder through the collision integral, enabling a more realistic description of experimental conditions. Crucially, the quantum kinetic equation captures resonant interband transitions between the valence and conduction bands—phenomena that lie beyond the reach of Boltzmann-based treatments. Similar resonant effects have recently been discussed in the context of a two-dimensional electron gas with spin-orbit coupling using the same analytical technique [53]. Looking ahead, we plan to extend this method to explore orbital effects of strong

magnetic fields in topological semimetals and flat-band systems [57–59], as well as to investigate the role of generic disorder in the quantization of the photogalvanic effect [60–62].

In conclusion, we have explored the nonlinear Hall effect in two-dimensional Dirac materials under the influence of an external in-plane magnetic field. Using the quantum kinetic equation, we identified two distinct contributions to the second harmonic response. The first, of geometric origin, arises intrinsically from the Berry curvature dipole; the second is magnetic-field-induced and increases quadratically with the field strength. Notably, the latter contribution exhibits a strong directional dependence, enabling the geometric response to be either enhanced or suppressed by adjusting the orientation of the applied field. Together, these findings suggest a practical and tunable tool for controlling nonlinear Hall phenomena in Dirac systems, offering clear experimental pathways for future investigation.

#### V. ACKNOWLEDGMENTS

We thank Leonid Golub for bringing several references to our attention and enlightening discussions. This work was financially supported by the National Science Foundation (NSF) grant DMR-2400484 (M. D.) and NSF-BSF Grant No. DMR-2023693 (M. K.). A. L. acknowledges the support from NSF Grant No. DMR-2452658 and H. I. Romnes Faculty Fellowship provided by the University of Wisconsin-Madison Office of the Vice Chancellor for Research and Graduate Education with funding from the Wisconsin Alumni Research Foundation. M. D. and A. L. have performed this work in part at Aspen Center for Physics, which is supported by the National Science Foundation grant PHY-2210452.

#### Appendix A: Linear anomalous Hall effect

Assuming that  $\alpha \ll v$ , we use Eq. (11) along with the definition (12) to evaluate *linear* Hall conductivity  $\sigma_{xy} = j_y/\mathcal{E}_x$ . Taking the limit  $T \rightarrow 0$ , we find

$$\sigma_{xy}^{(s)} = \left( \frac{sm e^2 v^2}{\pi \hbar} \right) \int_0^\infty \frac{k dk}{z_\omega^2 + 4b_{\mathbf{k}}^2} \int_0^{2\pi} \frac{d\phi}{2\pi} \sum_{\eta=1}^2 \delta(\mu - \epsilon_{\mathbf{k}s}^{(\eta)}), \quad (\text{A1})$$

where  $\mu$  is the chemical potential. We emphasize that integral in Eq. (A1) can be rewritten as the integral over the Berry curvature, after performing the integration by parts. In the simplest case  $\alpha = 0$ , the integral can be easily evaluated with the following result

$$[\sigma_{xy}]_{\alpha=0} = \left( \frac{m e^2}{\pi \hbar} \right) \frac{\mu \tau^2}{(1 - i\omega\tau)^2 + (2\mu\tau)^2}. \quad (\text{A2})$$

We consider the static limit  $\omega \rightarrow 0$  in the absence of disorder,  $\tau \rightarrow \infty$ , but keeping  $\omega\tau \ll 1$ . Then, setting  $\mu = m + 0$  in Eq. (A1), we readily recover the expression for the intrinsic

contribution to the anomalous Hall conductivity for a single valley:

$$[\sigma_{xy}^{(\text{int.})}]_{\alpha=0} = \left( \frac{e^2}{4\pi\hbar} \right) \text{sign}(s). \quad (\text{A3})$$

The subsequent summation over the valley index leads to the cancellation of the corresponding contributions, as guaranteed by the time-reversal symmetry. The second-order Hall effect, which is the main focus of our work, survives even in time-reversal-symmetric systems.

## Appendix B: Berry curvature dipole contribution

In this Appendix, we provide the details of the calculation of the integral in Eq. (23). We consider the following integral:

$$J_{\text{B.d.}} = - \int \frac{d^2\mathbf{k}}{(2\pi)^2} \frac{mv^2}{b_{\mathbf{k}}^3} \frac{\partial f(\epsilon_{\mathbf{k}})}{\partial k_x}. \quad (\text{B1})$$

In the low-temperature limit  $T \rightarrow 0$ , the Fermi distribution function can be approximated by the step function

$$f(\epsilon_{\mathbf{k}}) \approx \vartheta(\mu - \epsilon_{\mathbf{k}}). \quad (\text{B2})$$

Thus, the integration in Eq. (B1) is performed over the surface

$$\alpha k_x + \sqrt{m^2 + v^2 k^2} = \mu. \quad (\text{B3})$$

We will integrate over  $k_x$  and  $k_y$  separately. We start with integrating over  $k_y$  first by introducing a new variable

$$y = \sqrt{m^2 + v^2 k^2}. \quad (\text{B4})$$

It follows that

$$J_{\text{B.d.}} = \frac{mv}{2\pi^2} \int_{-\infty}^{\infty} \frac{[\alpha(\mu - \alpha k_x) + v^2 k_x] \vartheta(\mu - \alpha k_x - m_x) dk_x}{(\mu - \alpha k_x)^3 \sqrt{(\mu - \alpha k_x)^2 - m_x^2}}, \quad (\text{B5})$$

where  $m_x = \sqrt{m^2 + v^2 k_x^2}$ . We split Eq. (B5) into two integrals:

$$\begin{aligned} J_{\text{B.d.}}^{(+)} &= \frac{mv}{2\pi^2} \int_0^{\infty} \left( \alpha + \frac{v^2 k_x}{\mu - \alpha k_x} \right) \frac{\vartheta(\mu - \alpha k_x - m_x) dk_x}{(\mu - \alpha k_x)^2 \sqrt{(\mu - \alpha k_x)^2 - m_x^2}}, \\ J_{\text{B.d.}}^{(-)} &= \frac{mv}{2\pi^2} \int_0^{\infty} \left( \alpha - \frac{v^2 k_x}{\mu + \alpha k_x} \right) \frac{\vartheta(\mu + \alpha k_x - m_x) dk_x}{(\mu + \alpha k_x)^2 \sqrt{(\mu + \alpha k_x)^2 - m_x^2}}. \end{aligned}$$

Note that  $J_{\text{B.d.}}^{(+)} + J_{\text{B.d.}}^{(-)} = 0$  when we set  $\alpha = 0$ . In order to evaluate the first integral, we change the integration variable according to

$$k_x = q_x - \frac{\alpha\mu}{v^2 - \alpha^2}. \quad (\text{B6})$$

Given Eq. (B6), it also follows that

$$\begin{aligned} \alpha + \frac{v^2 k_x}{\mu - \alpha k_x} &= \frac{\alpha\mu + (v^2 - \alpha^2)k_x}{\mu - \alpha k_x} = \frac{(v^2 - \alpha^2)q_x}{\mu - \alpha k_x}, \\ \mu - \alpha k_x &= \frac{\mu^2}{v^2 - \alpha^2} - \alpha q_x \equiv \alpha(Q - q_x). \end{aligned} \quad (\text{B7})$$

Furthermore, we have

$$\begin{aligned} (\mu - \alpha k_x)^2 - m_x^2 &= \frac{\mu^2 v^2}{v^2 - \alpha^2} - m^2 - (v^2 - \alpha^2)q_x^2 \\ &\equiv (v^2 - \alpha^2)(\Lambda^2 - q_x^2), \end{aligned} \quad (\text{B8})$$

where

$$\Lambda = \frac{1}{\sqrt{v^2 - \alpha^2}} \sqrt{\frac{\mu^2 v^2}{v^2 - \alpha^2} - m^2} \equiv \frac{\gamma}{\sqrt{v^2 - \alpha^2}}. \quad (\text{B9})$$

Keeping in mind that  $\alpha < v$ , we note that

$$Q = \frac{v}{\alpha} \left( \frac{\mu v}{v^2 - \alpha^2} \right) > \Lambda. \quad (\text{B10})$$

It will be convenient to use the shorthand notation

$$u = \frac{\alpha}{\sqrt{v^2 - \alpha^2}}. \quad (\text{B11})$$

After we substitute these expressions into the integral and make a change of variables  $x = q_x \sqrt{v^2 - \alpha^2}$ , we have

$$\begin{aligned} J_{\text{B.d.}}^{(+)}(\alpha) &= \frac{mv(v^2 - \alpha^2)^{3/2}}{2\pi^2 \alpha^3} \int_{u\mu}^{\gamma} \frac{x dx}{\left[ \left( \frac{v}{\alpha} \right)^2 u\mu - x \right]^3 \sqrt{\gamma^2 - x^2}} \\ &= \frac{mv}{2\pi^2} \frac{(v^2 - \alpha^2)^{3/2}}{\alpha^3 \gamma^2} \int_{u\mu/\gamma}^1 \frac{q dq}{(a - q)^3 \sqrt{1 - q^2}} \end{aligned} \quad (\text{B12})$$

with  $a = v^2 u\mu / \alpha^2 \gamma$ . We note that

$$\begin{aligned} J_{\text{B.d.}}^{(-)}(\alpha) &= -J_{\text{B.d.}}^{(+)}(-\alpha) \\ &= -\frac{mv}{2\pi^2} \frac{(v^2 - \alpha^2)^{3/2}}{\alpha^3 \gamma^2} \int_{-u\mu/\gamma}^1 \frac{q dq}{(a + q)^3 \sqrt{1 - q^2}}, \end{aligned} \quad (\text{B13})$$

which follows from the definition (B6). Changing under the integral  $q \rightarrow -q$ , we find

$$\begin{aligned} J_{\text{B.d.}}(\alpha) &= J_{\text{B.d.}}^{(+)}(\alpha) + J_{\text{B.d.}}^{(-)}(\alpha) \\ &= \frac{mv}{2\pi^2} \frac{(v^2 - \alpha^2)^{3/2}}{\alpha^3 \gamma^2} \int_{-1}^1 \frac{q dq}{(a - q)^3 \sqrt{1 - q^2}} \\ &= \frac{mv}{2\pi^2} \frac{(v^2 - \alpha^2)^{3/2}}{\alpha^3 \gamma^2} \left[ \frac{3\pi a}{2(a^2 - 1)^{5/2}} \right]. \end{aligned} \quad (\text{B14})$$

This expression can be further simplified by using the following identities:

$$\begin{aligned} a^2 - 1 &= \frac{(\mu^2 v^2 + \alpha^2 m^2)(v^2 - \alpha^2)}{\alpha^2 [(\mu^2 - m^2)v^2 + m^2 \alpha^2]}, \\ a &= \frac{\mu v^2}{\alpha \sqrt{(\mu^2 - m^2)v^2 + m^2 \alpha^2}}. \end{aligned} \quad (\text{B15})$$

It then follows that

$$J_{\text{B.d.}}(\alpha) = \left( \frac{\gamma^2}{4\pi} \right) \frac{3\alpha\mu v^3 (v^2 - \alpha^2)}{(\mu^2 v^2 + m^2 \alpha^2)^{5/2}}. \quad (\text{B16})$$



We emphasize that this expression should be viewed as the leading-order contribution to the second harmonic at small  $\alpha$ . Taking the limit  $\alpha \ll v$  and  $m \ll \mu$ , we find

$$[J_{\text{B.d.}}]_{m \ll \mu}^{\alpha \ll v} \approx \frac{3}{4\pi} \left( \frac{m\alpha}{\mu^2} \right), \quad (\text{B17})$$

where we took into account that  $[\gamma]_{m \ll \mu} \approx \mu$ .

### Appendix C: Corrections to the Wigner distribution function in the presence of magnetic field and linear magnetoconductivity

In the presence of magnetic field, the right hand side of the kinetic equation (9) acquires an additional term

$$[\hat{w}_{\mathbf{q}\epsilon}^{(2)}]_{aa} = -\left(\frac{e}{\omega}\right) \frac{([\hat{\mathbf{v}}]_{aa} \cdot \vec{\mathcal{E}})}{z_{2\omega}} \left[ \hat{w}_{\mathbf{q}\epsilon+\frac{\omega}{2}}^{(1)} - \hat{w}_{\mathbf{q}\epsilon-\frac{\omega}{2}}^{(1)} \right]_{aa} - \left(\frac{e}{2\omega}\right) \frac{([\hat{\mathbf{v}}]_{a\bar{a}} \cdot \vec{\mathcal{E}})}{z_{2\omega}} \left[ \hat{w}_{\mathbf{q}\epsilon+\frac{\omega}{2}}^{(1)} - \hat{w}_{\mathbf{q}\epsilon-\frac{\omega}{2}}^{(1)} \right]_{\bar{a}a} - \left(\frac{e}{2\omega}\right) \frac{([\hat{\mathbf{v}}]_{\bar{a}a} \cdot \vec{\mathcal{E}})}{z_{2\omega}} \left[ \hat{w}_{\mathbf{q}\epsilon+\frac{\omega}{2}}^{(1)} - \hat{w}_{\mathbf{q}\epsilon-\frac{\omega}{2}}^{(1)} \right]_{a\bar{a}}.$$

Here,  $z_{2\omega} = -2i\omega + 1/\tau$ . Similarly, for the off-diagonal elements we find

$$[\hat{w}_{\mathbf{k}\epsilon}^{(2)}]_{12} = -\left(\frac{e}{2\omega}\right) \left( \frac{[\hat{\mathbf{v}}]_{12} \cdot \vec{\mathcal{E}}}{z_{2\omega} - 2ib_{\mathbf{q}}} \right) \sum_{a=1}^2 \left[ \hat{w}_{\mathbf{q}\epsilon+\frac{\omega}{2}}^{(1)} - \hat{w}_{\mathbf{q}\epsilon-\frac{\omega}{2}}^{(1)} \right]_{aa},$$

$$[\hat{w}_{\mathbf{k}\epsilon}^{(2)}]_{21} = -\left(\frac{e}{2\omega}\right) \left( \frac{[\hat{\mathbf{v}}]_{21} \cdot \vec{\mathcal{E}}}{z_{2\omega} + 2ib_{\mathbf{q}}} \right) \sum_{a=1}^2 \left[ \hat{w}_{\mathbf{q}\epsilon+\frac{\omega}{2}}^{(1)} - \hat{w}_{\mathbf{q}\epsilon-\frac{\omega}{2}}^{(1)} \right]_{aa}.$$

We employ these formulas in the derivation of the expression (32) of the main text.

Equations (30)-(31) and (C1) allow us to estimate *linear* magnetoconductivity. We assume for simplicity that the magnetic field is weak and parameter  $\beta$  is small, i.e.  $\beta k_F^2 \ll m$ . This approximation allows us to switch from integration over  $\mathbf{k}$  to integration over  $\mathbf{q}$  in the expression for the current density (12). With the help of Eqs. (30)-(31) and (C1), we obtain three different contributions to the current, which are propor-

$-\beta \left\{ \mathbf{k} \hat{\sigma}_z, \vec{\nabla} \hat{w}_{\mathbf{k}\epsilon}(t) \right\}_+ / 2$ . Because of this term, the corresponding expressions for the first-order corrections to the Wigner distribution function can be compactly expressed in terms of the matrix elements of the velocity operators as follows:

$$[\hat{w}_{\mathbf{q}\epsilon}^{(1)}]_{aa} = -\left(\frac{e}{\omega z_{2\omega}}\right) ([\hat{\mathbf{v}}]_{aa} \cdot \vec{\mathcal{E}}) \left[ \hat{w}_{\mathbf{q}\epsilon+\frac{\omega}{2}}^{(0)} - \hat{w}_{\mathbf{q}\epsilon-\frac{\omega}{2}}^{(0)} \right]_{aa},$$

$$[\hat{w}_{\mathbf{q}\epsilon}^{(1)}]_{a\bar{a}} = -\left(\frac{e}{2\omega}\right) \frac{([\hat{\mathbf{v}}]_{a\bar{a}} \cdot \vec{\mathcal{E}})}{(z_{2\omega} - 2ib_{\mathbf{q}})} \sum_{a=1}^2 \left[ \hat{w}_{\mathbf{q}\epsilon+\frac{\omega}{2}}^{(0)} - \hat{w}_{\mathbf{q}\epsilon-\frac{\omega}{2}}^{(0)} \right]_{aa}. \quad (\text{C1})$$

Here the matrix elements of the velocity operators are given by Eqs. (30)-(31) of the main text.

The second-order corrections to the WDF can be found similarly to Eq. (C1). For the correction to the first diagonal element of the WDF, we have

tional to  $[\hat{v}_y]_{22}[\hat{v}_x]_{22}$ ,  $[\hat{v}_y]_{22}[\hat{v}_x]_{12}$  and  $[\hat{v}_y]_{22}[\hat{v}_x]_{21}$ . It is straightforward to show that the contribution to the *linear* transverse current  $j_y^{(1)}$  from the last two terms is proportional to  $sB_x B_y$ , which vanishes upon the summation over the valley index  $s$ . For the product of the diagonal components of the velocity averaged over the directions of  $\mathbf{n} = \mathbf{q}/q$ , we find

$$\langle [\hat{v}_y]_{22}[\hat{v}_x]_{22} \rangle_{\mathbf{n}} = \frac{\alpha\beta m}{b_{\mathbf{q}}} g\mu_B B_y + s \left( \frac{\beta m}{b_{\mathbf{q}}} \right)^2 (g\mu_B)^2 B_x B_y. \quad (\text{C2})$$

Upon the subsequent summation over  $s$  the contribution from the second term vanishes, and we conclude that the only non-zero contribution to the current originates from the first term so that

$$j_y^{(1)} \propto \alpha\beta g\mu_B B_y \mathcal{E}_x. \quad (\text{C3})$$

We leave the detailed study of the linear magneto-transport, including orbital effects [63], to future work.

- 
- [1] A. A. Abrikosov, *Fundamentals of the Theory of Metals* (North-Holland, Amsterdam, 1988).
  - [2] M.-C. Chang and Q. Niu, Berry phase, hyperorbits, and the Hofstadter spectrum, *Phys. Rev. Lett.* **75**, 1348 (1995).
  - [3] G. Sundaram and Q. Niu, Wave-packet dynamics in slowly perturbed crystals: Gradient corrections and Berry-phase effects, *Phys. Rev. B* **59**, 14915 (1999).
  - [4] F. D. M. Haldane, Berry curvature on the Fermi surface: Anomalous Hall effect as a topological Fermi-liquid property, *Phys. Rev. Lett.* **93**, 206602 (2004).
  - [5] G. Sundaram and Q. Niu, Wave-packet dynamics in slowly perturbed crystals: Gradient corrections and berry-phase effects, *Phys. Rev. B* **59**, 14915 (1999).
  - [6] D. Xiao, M.-C. Chang, and Q. Niu, Berry phase effects on electronic properties, *Rev. Mod. Phys.* **82**, 1959 (2010).
  - [7] N. Nagaosa, J. Sinova, S. Onoda, A. H. MacDonald, and N. P. Ong, Anomalous hall effect, *Rev. Mod. Phys.* **82**, 1539 (2010).
  - [8] M. Papaj and L. Fu, Magnus Hall effect, *Phys. Rev. Lett.* **123**, 216802 (2019).
  - [9] D. Mandal, K. Das, and A. Agarwal, Magnus Nernst and thermal Hall effect, *Phys. Rev. B* **102**, 205414 (2020).
  - [10] Z. Z. Du, H.-Z. Lu, and X. C. Xie, Nonlinear Hall effects, *Nature Reviews Physics* **3**, 744 (2021).
  - [11] T. Holder, D. Kaplan, and B. Yan, Consequences of time-reversal-symmetry breaking in the light-matter interaction: Berry curvature, quantum metric, and diabatic motion, *Phys.*

- Rev. Res. **2**, 033100 (2020).
- [12] J. Ahn, G.-Y. Guo, and N. Nagaosa, Low-frequency divergence and quantum geometry of the bulk photovoltaic effect in topological semimetals, *Phys. Rev. X* **10**, 041041 (2020).
- [13] P. Bhalla, A. H. MacDonald, and D. Culcer, Resonant photovoltaic effect in doped magnetic semiconductors, *Phys. Rev. Lett.* **124**, 087402 (2020).
- [14] H. Watanabe and Y. Yanase, Chiral photocurrent in parity-violating magnet and enhanced response in topological antiferromagnet, *Phys. Rev. X* **11**, 011001 (2021).
- [15] J. B. Khurgin, Current induced second harmonic generation in semiconductors, *Applied Physics Letters* **67**, 1113 (1995).
- [16] E. J. König and A. Levchenko, Quantum kinetics of anomalous and nonlinear hall effects in topological semimetals, *Annals of Physics* **435**, 168492 (2021), special issue on Philip W. Anderson.
- [17] E. Deyo, L. E. Golub, E. L. Ivchenko, and B. Spivak, Semiclassical theory of the photogalvanic effect in non-centrosymmetric systems, arXiv:0904.1917 (2009).
- [18] I. Sodemann and L. Fu, Quantum nonlinear Hall effect induced by Berry curvature dipole in time-reversal invariant materials, *Phys. Rev. Lett.* **115**, 216806 (2015).
- [19] S. Nandy and I. Sodemann, Symmetry and quantum kinetics of the nonlinear Hall effect, *Phys. Rev. B* **100**, 195117 (2019).
- [20] T. Low, Y. Jiang, and F. Guinea, Topological currents in black phosphorus with broken inversion symmetry, *Phys. Rev. B* **92**, 235447 (2015).
- [21] J. I. Facio, D. Efremov, K. Koepernik, J.-S. You, I. Sodemann, and J. van den Brink, Strongly enhanced Berry dipole at topological phase transitions in BiTeI, *Phys. Rev. Lett.* **121**, 246403 (2018).
- [22] J.-S. You, S. Fang, S.-Y. Xu, E. Kaxiras, and T. Low, Berry curvature dipole current in the transition metal dichalcogenides family, *Phys. Rev. B* **98**, 121109 (2018).
- [23] Y. Zhang, Y. Sun, and B. Yan, Berry curvature dipole in Weyl semimetal materials: An ab initio study, *Phys. Rev. B* **97**, 041101 (2018).
- [24] Z. Z. Du, C. M. Wang, H.-Z. Lu, and X. C. Xie, Band signatures for strong nonlinear Hall effect in bilayer WTe<sub>2</sub>, *Phys. Rev. Lett.* **121**, 266601 (2018).
- [25] Y. Zhang, J. van den Brink, C. Felser, and B. Yan, Electrically tuneable nonlinear anomalous Hall effect in two-dimensional transition-metal dichalcogenides WTe<sub>2</sub> and MoTe<sub>2</sub>, *2D Materials* **5**, 044001 (2018).
- [26] C. Aversa and J. E. Sipe, Nonlinear optical susceptibilities of semiconductors: Results with a length-gauge analysis, *Phys. Rev. B* **52**, 14636 (1995).
- [27] J. E. Sipe and A. I. Shkrebtii, Second-order optical response in semiconductors, *Phys. Rev. B* **61**, 5337 (2000).
- [28] M. Glazov and S. Ganichev, High frequency electric field induced nonlinear effects in graphene, *Physics Reports* **535**, 101 (2014).
- [29] T. Morimoto and N. Nagaosa, Topological nature of nonlinear optical effects in solids, *Science Advances* **2**, e1501524 (2016).
- [30] N. Sirica, R. I. Tobey, L. X. Zhao, G. F. Chen, B. Xu, R. Yang, B. Shen, D. A. Yarotski, P. Bowlan, S. A. Trugman, J.-X. Zhu, Y. M. Dai, A. K. Azad, N. Ni, X. G. Qiu, A. J. Taylor, and R. P. Prasankumar, Tracking ultrafast photocurrents in the Weyl semimetal TaAs using THz emission spectroscopy, *Phys. Rev. Lett.* **122**, 197401 (2019).
- [31] Z.-H. Dong, H. Yang, and Y. Zhang, Enhanced nonlinear Hall effect by Cooper pairs near the superconducting phase transition, *Phys. Rev. B* **111**, 155120 (2025).
- [32] Q. Ma, S.-Y. Xu, H. Shen, D. MacNeill, V. Fatemi, T.-R. Chang, A. M. Mier Valdivia, S. Wu, Z. Du, C.-H. Hsu, S. Fang, Q. D. Gibson, K. Watanabe, T. Taniguchi, R. J. Cava, E. Kaxiras, H.-Z. Lu, H. Lin, L. Fu, N. Gedik, and P. Jarillo-Herrero, Observation of the nonlinear Hall effect under time-reversal-symmetric conditions, *Nature* **565**, 337 (2019).
- [33] A. Tiwari, F. Chen, S. Zhong, E. Drueke, J. Koo, A. Kaczmarek, C. Xiao, J. Gao, X. Luo, Q. Niu, Y. Sun, B. Yan, L. Zhao, and A. W. Tsen, Giant *c*-axis nonlinear anomalous Hall effect in Td-MoTe<sub>2</sub> and WTe<sub>2</sub>, *Nature Nanotechnology* **12**, 2049 (2021).
- [34] M.-S. Qin, P.-F. Zhu, X.-G. Ye, W.-Z. Xu, Z.-H. Song, J. Liang, K. Liu, and Z.-M. Liao, Strain tunable Berry curvature dipole, orbital magnetization and nonlinear Hall effect in WSe<sub>2</sub> monolayer, *Chinese Physics Letters* **38**, 017301 (2021).
- [35] D. Kumar, C.-H. Hsu, R. Sharma, T.-R. Chang, P. Yu, J. Wang, G. Eda, G. Liang, and H. Yang, Room-temperature nonlinear Hall effect and wireless radiofrequency rectification in Weyl semimetal TaIrTe<sub>4</sub>, *Nature Nanotechnology* **16**, 421 (2021).
- [36] P. He, H. Isobe, D. Zhu, C.-H. Hsu, L. Fu, and H. Yang, Quantum frequency doubling in the topological insulator Bi<sub>2</sub>Se<sub>3</sub>, *Nature Communications* **12**, 698 (2021).
- [37] M. Huang, Z. Wu, J. Hu, X. Cai, E. Li, L. An, X. Feng, Z. Ye, N. Lin, K. T. Law, and N. Wang, Giant nonlinear Hall effect in twisted bilayer WSe<sub>2</sub>, *National Science Review* **10**, nwac232 (2022).
- [38] C. Xiao, W. Wu, H. Wang, Y.-X. Huang, X. Feng, H. Liu, G.-Y. Guo, Q. Niu, and S. A. Yang, Time-reversal-even nonlinear current induced spin polarization, *Phys. Rev. Lett.* **130**, 166302 (2023).
- [39] S. Dzsaber, X. Yan, M. Taupin, G. Eguchi, A. Prokofiev, T. Shiroka, P. Blaha, O. Rubel, S. E. Grefe, H.-H. Lai, Q. Si, and S. Paschen, Giant spontaneous Hall effect in a nonmagnetic Weyl-Kondo semimetal, *Proceedings of the National Academy of Sciences* **118**, e2013386118 (2021).
- [40] H.-H. Lai, S. E. Grefe, S. Paschen, and Q. Si, Weyl-Kondo semimetal in heavy-fermion systems, *Proceedings of the National Academy of Sciences* **115**, 93 (2018), <https://www.pnas.org/doi/pdf/10.1073/pnas.1715851115>.
- [41] M. Braß, J. M. Tomczak, and K. Held, Weyl nodes in Ce<sub>3</sub>Bi<sub>4</sub>Pd<sub>3</sub> revealed by dynamical mean-field theory, *Phys. Rev. Res.* **6**, 033227 (2024).
- [42] S. Sur, L. Chen, Y. Wang, C. Setty, S. Paschen, and Q. Si, Fully nonequilibrium Hall response from Berry curvature, arXiv:2411.16675 (2025).
- [43] V. M. Edel'shtein, Second-harmonic generation in two-dimensional systems without inversion centers, *Sov. Phys. - JETP* **68**, 1446 (1988).
- [44] L. I. Magarill, Photogalvanic effect in two-dimensional electronic systems in parallel magnetic field, *Sov. Phys. - Solid State* **32**, 3558 (1990).
- [45] A. P. Dmitriev, S. A. Emel'yanov, S. V. Ivanov, P. Kop'ev, Y. V. Terent'ev, and I. D. Yaroshetskii, Photogalvanic effect in two-dimensional electronic systems in parallel magnetic field, *Sov. Phys. - JETP Lett.* **54**, 273 (1991).
- [46] Z. Z. Du, C. M. Wang, H.-P. Sun, H.-Z. Lu, and X. C. Xie, Quantum theory of the nonlinear Hall effect, *Nature Communications* **12**, 5038 (2021).
- [47] J. Liu, W. Duan, and L. Fu, Two types of surface states in topological crystalline insulators, *Phys. Rev. B* **88**, 241303 (2013).
- [48] M. Serbyn and L. Fu, Symmetry breaking and Landau quantization in topological crystalline insulators, *Phys. Rev. B* **90**, 035402 (2014).
- [49] T. H. Hsieh, H. Lin, J. Liu, W. Duan, A. Bansil, and L. Fu, Topological crystalline insulators in the snite material class, Na-

- ture Communications **3**, 982 (2012).
- [50] S. Fang, S. Carr, M. A. Cazalilla, and E. Kaxiras, Electronic structure theory of strained two-dimensional materials with hexagonal symmetry, *Phys. Rev. B* **98**, 075106 (2018).
  - [51] J.-S. You, S. Fang, S.-Y. Xu, E. Kaxiras, and T. Low, Berry curvature dipole current in the transition metal dichalcogenides family, *Phys. Rev. B* **98**, 121109 (2018).
  - [52] A. V. Shytov, E. G. Mishchenko, H.-A. Engel, and B. I. Halperin, Small-angle impurity scattering and the spin Hall conductivity in two-dimensional semiconductor systems, *Phys. Rev. B* **73**, 075316 (2006).
  - [53] M. Dzero, J. Hasan, and A. Levchenko, Resonant second harmonic generation in a two-dimensional electron system, *arXiv:2411.08947* (2024).
  - [54] P. Bhalla, K. Das, D. Culcer, and A. Agarwal, Resonant second-harmonic generation as a probe of quantum geometry, *Phys. Rev. Lett.* **129**, 227401 (2022).
  - [55] L. E. Golub, E. L. Ivchenko, and B. Spivak, Semiclassical theory of the circular photogalvanic effect in gyrotropic systems, *Phys. Rev. B* **102**, 085202 (2020).
  - [56] E. J. König, M. Dzero, A. Levchenko, and D. A. Pesin, Gyrotropic Hall effect in Berry-curved materials, *Phys. Rev. B* **99**, 155404 (2019).
  - [57] T. Morimoto, S. Zhong, J. Orenstein, and J. E. Moore, Semi-classical theory of nonlinear magneto-optical responses with applications to topological Dirac/Weyl semimetals, *Phys. Rev. B* **94**, 245121 (2016).
  - [58] G. Bednik and V. Kozii, Magnetic field induces giant nonlinear optical response in Weyl semimetals, *Phys. Rev. B* **109**, 045106 (2024).
  - [59] V. Hassanzade and V. Kozii, Strong photogalvanic effect in Weyl materials due to magnetic resonances (2025).
  - [60] F. de Juan, A. G. Grushin, T. Morimoto, and J. E. Moore, Quantized circular photogalvanic effect in Weyl semimetals, *Nature Communications* **8**, 15995 (2017).
  - [61] F. de Juan, Y. Zhang, T. Morimoto, Y. Sun, J. E. Moore, and A. G. Grushin, Difference frequency generation in topological semimetals, *Phys. Rev. Res.* **2**, 012017 (2020).
  - [62] A. Avdoshkin, V. Kozii, and J. E. Moore, Interactions remove the quantization of the chiral photocurrent at Weyl points, *Phys. Rev. Lett.* **124**, 196603 (2020).
  - [63] V. Sunko, C. Liu, M. Vila, I. Na, Y. Tang, V. Kozii, S. M. Griffin, J. E. Moore, and J. Orenstein, Linear magnetoconductivity as a DC probe of time-reversal symmetry breaking, *arXiv:2310.15631* (2023).